PHYSICAL REVIEW B VOLUME 2, NUMBER 10 15 NOVEMBER 1970

Anisotropic Heat Conduction in Cubic Crystals in the Boundary Scattering Regime*

A. K. McCurdy, H. J. Maris, and C. Elbaum
Physics Department, Brown University, Providence, Rhode Island 02912
(Received 17 February 1970; revised manuscript received 22 July 1970)

The thermal conductivities of single crystals of silicon and of calcium fluoride have been measured in the temperature range 3–40 °K and 2.5–30 °K, respectively. For samples in the form of square cross-section rods, the conductivity in the boundary scattering regime was found to depend on the orientation of the rod axis, the variation being as much as 50% for silicon. This anisotropy is accounted for in terms of phonon focusing due to the fact that in elastically anisotropic crystals the phonon phase and group velocities are, in general, not collinear. Casimir's theory of the thermal conduction in the boundary scattering regime has been generalized to include the effects of focusing; the predictions of this generalized theory are in quantitative agreement with the experimental results. It is predicted that anisotropic thermal conductivity in the boundary scattering regime is a general property of elastically anisotropic cubic crystals.

I. INTRODUCTION

At sufficiently low temperatures the mean free path of thermal phonons in a dielectric crystal of high purity and perfection becomes limited by the boundaries of the sample.[1] A theory of the thermal conductivity applicable to this temperature range was first developed by Casimir,[2] whose result may be expressed in the equivalent forms

$$\kappa = (2\pi^2 k_B^4/15\hbar^3)\langle s^{-2}\rangle \Lambda_c T^3 \ , \tag{1}$$

$$\kappa = \tfrac{1}{3} C(\langle s^{-2}\rangle/\langle s^{-3}\rangle)\Lambda_c \ , \tag{2}$$

where $\langle s^{-2}\rangle$ and $\langle s^{-3}\rangle$ are, respectively, averages of the inverse square and inverse cube of the phonon phase velocity, T is the temperature, and C the specific heat per unit volume. Λ_c, the Casimir length, may be regarded as the effective phonon mean free path. For a circular cross-section rod, Λ_c is equal to the rod diameter and for a square rod of side D

$$\Lambda_c = 1.12D \ . \tag{3}$$

Experimental measurements of the thermal conductivity under conditions where the Casimir theory should apply were first performed by de Haas and Biermasz[3] on quartz and potassium chloride. These experiments and more recent work are in agreement with Eqs. (1) and (2) in that the conductivity is generally found to vary with temperature as T^3 and increases linearly with the transverse dimensions of the crystal. The thermal conductivity calculated from this theory is also of the same order of magnitude as measured experimentally, but quantitative agreement between theoretical predictions and experimental results is often lacking. There are several possible reasons for this and in particular the following points have been made:

Length correction. Casimir's theory assumes that the sample has a length very much greater than its transverse dimensions. A correction to take account of the finite ratio of sample length to sample width was derived by Berman and co-workers.[4,5] This effect reduces the conductivity below that predicted by Casimir.

Specular reflection. Casimir assumed that the walls of the sample acted as diffuse scatterers of phonons, i.e., a phonon striking the surface of the crystal would be reradiated with random direction. However, in general, one expects that a certain fraction of the phonons will be specularly reflected. It has been shown[4] that this effect increases the conductivity by a factor

$$(1+p)/(1-p) \ .$$

p varies with the surface condition and may also depend upon temperature. The variation with temperature occurs because with decreasing temperature the average phonon wavelength increases and consequently a surface of given roughness appears smoother.

In this paper we describe another way in which the conductivity may differ from the predictions of Eqs. (1) and (2). Heat-pulse studies[6] have shown that when phonons are excited in a given region of an elastically anisotropic crystal, the energy flow will be enhanced or focused in some directions and decreased in others even if the angular distribution of wave vectors is uniform. This enhancement or decrease arises because the group velocity $\vec{v}$ is not generally in the same direction as the wave vector $\vec{k}$ or the phase velocity $\vec{s}$. One therefore expects that the thermal conduction in the boundary scattering regime should depend on the direction of the rod axis and should be larger than average when the axis is parallel to a crystallographic direction in which the energy flow is enhanced. This is shown schematically in Fig. 1.

At temperatures much less than the Debye temperature most of the thermal energy of a solid is contained in the transverse modes because of their

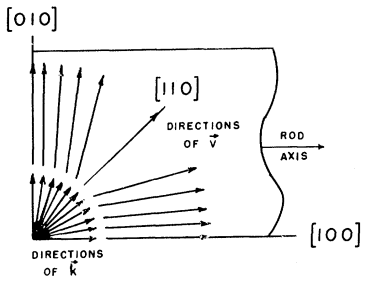

FIG. 1. Schematic diagram showing phonon focusing. A uniform angular distribution of wave vectors is shown. The deviation in direction of the group velocity vectors $\vec{v}$ relative to their corresponding wave vectors $\vec{k}$ is such that there are more phonons traveling nearly parallel to the rod axis than there would be for an isotropic solid.

lower velocity. Thus, one expects that transverse phonons will make the major contribution to the heat conduction. It follows that, if focusing is indeed important, an enhanced conductivity should occur for those directions in which transverse phonons are most strongly focused. To investigate this possibility we have measured the conductivity in several differently oriented rods of silicon and calcium fluoride. The experimental procedure and results are described in Sec. II. In Sec. III, Casimir's theory is generalized to allow for phonon focusing, and in Sec. IV, we compare the predictions of this theory with the experimental results.

II. EXPERIMENTAL PROCEDURE

The thermal conductivity was measured in a cryostat of fairly conventional design using liquid helium as a coolant. The temperature gradient along the sample was determined using an annealed Au-0.02 at.%-Fe versus Chromel P differential thermocouple.[7] The thermocouple junctions were fastened to knife-edge clamps of high-conductivity copper which were mounted on the specimen at approximately equal distances from the heat source and sink. The output of the thermocouple was measured by a Keithley model 148 nanovoltmeter. Allen-Bradley $\frac{1}{10}$-W carbon resistors located on the thermocouple clamps were used to measure the sample temperature. These resistors were calibrated against a germanium thermometer (Texas Instruments Model 106) from 4 to 40 °K and against the vapor pressure of helium below 4 °K. The output of the thermocouple, the current and the voltage applied to the heater, and the output of the thermometers were continuously monitored on a Leeds and Northrup 12-point Speedomax recorder. The over-all accuracy of the thermal conductivity measurement is estimated to be ±4%.

All samples were prepared from a p-type silicon single crystal supplied by the Texas Instruments Company. The room-temperature electrical resistivity of the crystal was approximately 200 Ω cm and the dislocation density was less than 500 cm^{-2}. The dimensions and orientations of the various samples are shown in Table I. The surfaces of all samples including end faces were abraded using 200-J grade emery cloth supplied by the Behr Manning Company. The four square cross-section samples were abraded simultaneously to achieve as similar surface conditions as possible. Surfaces of the two rectangular cross-section samples were prepared in the same way. For the square cross-section samples, the distance between the heater and sink was 2.9 cm and between the thermocouple junctions 1.63 cm. The corresponding distances for the rectangular cross-section samples were 3.5 and 2.22 cm, respectively.

Results for the square samples are shown in Fig. 2 and for the two rectangular samples in Fig. 3. The thermal conductivity of all six silicon samples agreed to within experimental uncertainty at 40 °K, but they had significantly different conductivities at lower temperatures. Table I lists the conductivities at 3 °K for all samples. An effective mean free path Λ_{expt} has been calculated from the conductivity at 3 °K and this is also shown in Table I. This mean free path was determined using the relation

$$\Lambda_{expt} = 3\kappa_{expt}\langle s^{-3}\rangle/(C\langle s^{-2}\rangle) \ , \qquad (4)$$

where κ_{expt} is the experimental thermal conductivity. $\langle s^{-2}\rangle/\langle s^{-3}\rangle$ was calculated using the elastic constants and density given in Table II and was found to be 5.66×10^5 cm sec^{-1}. For the square samples, Λ_{expt} has been expressed in units of the side dimension, and should therefore be 1.12 according to Casimir's theory. For the rectangular cross-section samples, the mean free path is expressed in units of the geometric mean of the two side dimensions.

Detailed measurements of the thermal conductivity in silicon as a function of the direction of heat flow have previously been reported by Hurst and Frankl.[8] They also found that in the boundary scattering regime, the conductivity of ⟨100⟩ axis rods was greater than that of rods with ⟨110⟩ or ⟨111⟩ axes. Quantitative comparison between their results and ours is somewhat complicated because their samples did not have the same ratios of length to width as ours. However, when these differences are taken into account the two sets of data appear to be in essential agreement.

Calcium Fluoride

The samples were single crystals of "optical grade" material supplied by the Harshaw Chemical Company. The orientations and dimensions are listed in Table I. The surface of all samples were prepared in the same way as the silicon samples. Measurements of thermal conductivity were made from 2.5 to 30 °K and these results are shown in

TABLE I. Summary of experimental and theoretical results for silicon and calcium fluoride. For the rectangular cross-section rods the orientation of the wide face is denoted by an asterisk. The mean free paths are given in units of the geometric mean of the side dimensions of the rods. Λ_{theor}, Λ_{corr}, and Λ_{expt} are defined in the text. Cross-sectional dimensions accurate to ± 0.01 mm.

Material	Rod axis	Side faces	Dimensions (mm)	κ at 3 °K (W cm^{-1} °K^{-1})	Λ_{theor}	Λ_{corr}	V_{expt} ± 4%
Silicon	⟨100⟩	{100}	31×2.93×2.93	1.24	1.86	1.45	1.41
	⟨100⟩	{110}	37×2.93×2.93	1.16	1.84	1.43	1.32
	⟨110⟩	{100} {110}	37×2.93×2.93	0.87	1.29	1.06	0.98
	⟨111⟩	{110} {112}	37×2.93×2.93	0.81	1.09	0.98	0.91
	⟨110⟩	{100}* {110}	38×6.38×1.85	1.17	1.49	1.14	1.13
	⟨110⟩	{110}* {100}	38×6.38×1.85	0.88	1.02	0.88	0.86
Calcium fluoride	⟨100⟩	{100}	36×4.00×4.00	2.11	0.98	0.90	0.86
	⟨110⟩	{100} {110}	36×4.00×4.00	2.76	1.30	1.12	1.12
	⟨111⟩	{110} {112}	36×4.00×4.00	3.03	1.45	1.24	1.23

Fig. 4. In all of these experiments, the distance between the clamps was 2.00 cm and between the heater and sink 3.3 cm. The results for the conductivity at 3 °K are shown in Table I. The effective experimental mean free path was calculated in the same way as for silicon. The value of $\langle s^{-2}\rangle/\langle s^{-3}\rangle$ was found to be[9] 3.88×10^5 cm sec^{-1}.

III. THEORY

In this section we generalize Casimir's theory to allow for phonon focusing effects. Consider a rod of length L having uniform cross section (Fig. 5). Let us specify any point on the surface of the rod by a coordinate X_1 measured around the circumference and a coordinate X_3 measured along the rod

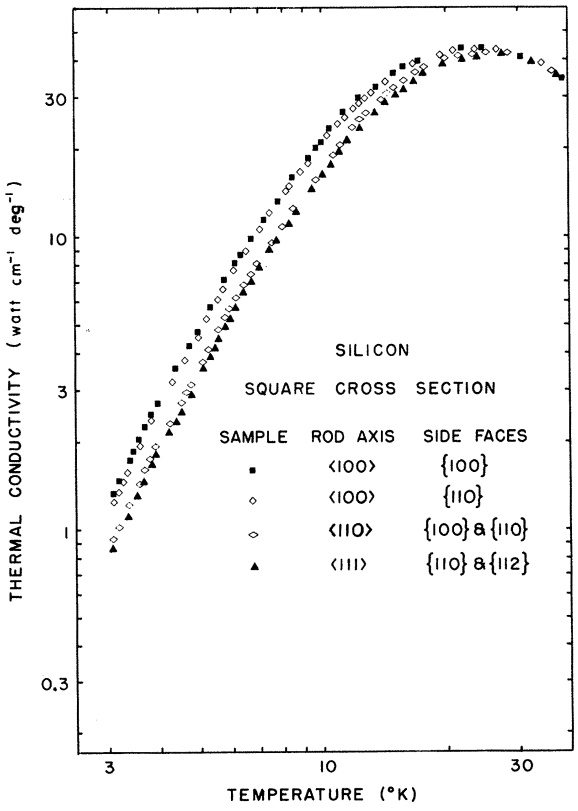

FIG. 2. Thermal conductivity of four square cross-section samples of silicon. The dimensions of the samples are given in Table I.

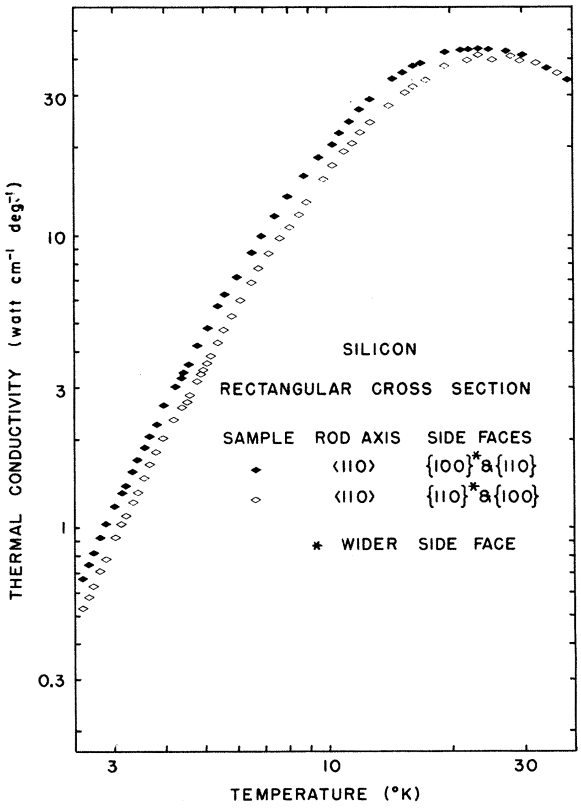

FIG. 3. Thermal conductivity of two rectangular samples of silicon. The dimensions of the samples are given in Table I.

TABLE II. Theoretical mean free paths Λ_{theor} for square cross-section infinite length rods of some cubic crystals. $\langle 100\rangle$-{100} and $\langle 100\rangle$-{110} denote $\langle 100\rangle$ axis rods with {100} and {110} side faces, respectively.

Crystal	Elastic constants (10^{11} dynes cm^{-2}) c_{11}	c_{12}	c_{44}	ρ (g cm^{-3})	$\langle s^{-2}\rangle/\langle s^{-3}\rangle$ (km sec^{-1})	Λ_{theor} (in units of side dimension D) $\langle 100\rangle$-{100}	$\langle 100\rangle$-{110}	$\langle 110\rangle$	$\langle 111\rangle$	Specific heat C_{theor} at 1 °K erg cm^{-3}
Si	16.77[a]	6.50	8.04	2.3301	5.66	1.86	1.84	1.29	1.09	5.91
CaF_2	17.4[b]	5.60	3.59	3.211	3.88	0.98	0.98	1.30	1.45	17.6
C	107.6[c]	12.5	57.6	3.512	13.08	1.55	1.55	1.11	1.13	0.505
LiF	12.46[d]	4.24	6.49	2.646	4.76	1.80	1.78	1.28	1.10	10.0
NaF	10.85[e]	2.29	2.90	2.851	3.64	1.01	1.01	1.33	1.42	22.2
NaCl	5.75[f]	0.99	1.33	2.214	2.88	1.05	1.05	1.23	1.43	43.9
KCl	4.83[g]	0.54	0.66	2.038	2.28	1.57	1.56	1.18	1.22	80.9

[a]H. J. McSkimin and P. Andreatch, J. Appl. Phys. 35, 2161 (1964).
[b]D. R. Huffmann and M. H. Norwood, Phys. Rev. 117, 709 (1960).
[c]H. J. McSkimin and W. L. Bond, Phys. Rev. 105, 116 (1957).
[d]C. V. Briscoe and C. F. Squire, Phys. Rev. 106, 1175 (1957).
[e]J. T. Lewis, A. Lehoczsky, and C. V. Briscoe, Phys. Rev. 161, 877 (1967).
[f]W. C. Overton and R. J. Swim, Phys. Rev. 84, 758 (1951).
[g]M. H. Norwood and C. V. Briscoe, Phys. Rev. 112, 45 (1958).

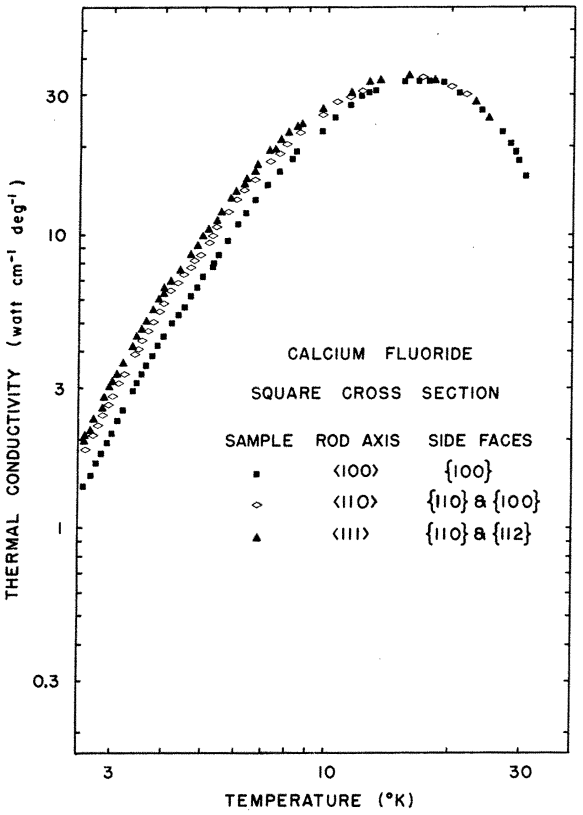

FIG. 4. Thermal conductivity of three square cross-section samples of calcium fluoride. The dimensions of the samples are given in Table I.

axis. The heat flow is thus in the X_3 direction. To calculate the conductivity we make three assumptions: (a) The surfaces of the rod radiate and absorb phonons as though they are perfectly "black". This assumption is the same as that made by Casimir. (b) The isothermals are planes normal to the X_3 axis. For a rod with cross section of arbitrary shape and with the X_3 direction being an arbitrary crystallographic direction this assumption is not generally valid. A sufficient condition for this assumption to be valid is that there be a mirror symmetry plane normal to the rod axis. For cubic crystals this condition is fulfilled for heat flow in the $\langle 100\rangle$ or $\langle 110\rangle$ directions. There is no mirror

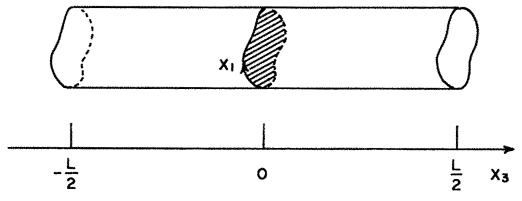

FIG. 5. Coordinate system used in calculating the conductivity. The shaded area indicates the plane $X_3 = 0$.

plane normal to the ⟨111⟩ direction but the resulting error is expected to be small. Further comments on this point are given in Sec. IV. (c) The temperature gradient along the rod is assumed to be uniform. For an infinitely long rod this assumption is rigorously valid. In the case of a finite length rod, however, one expects that the temperature gradient will be slightly greater near the ends of the rod.[4] One can show that the fractional error introduced into the conductivity by this assumption is of the order $(D/L)^2$ which, in the present experiments at least, is small. The "length correction" to the conductivity referred to in the Introduction is of order D/L.

Consider some element of surface area dS near the point (X_1, X_3). Let $\vec{n}(X_1)$ be a unit vector normal to the surface at this point and directed towards the interior. Then the number of phonons with wave vector $\vec{k}$ and polarization j leaving this element of surface per unit time is

$$\vec{n}(X_1)\cdot\vec{v}(\vec{k}j)N(\vec{k}jX_3)\,dS \quad ,$$

where $\vec{v}(\vec{k}j)$ is the group velocity of phonon $\vec{k}j$ and $N(\vec{k}jX_3)$ is the Bose-Einstein distribution function corresponding to the temperature $T(X_3)$ at the surface element. Thus

$$N(\vec{k}jX_3)=\{\exp[\hbar\omega(\vec{k}j)/k_BT(X_3)]-1\}^{-1} \quad , \tag{5}$$

where $\omega(\vec{k}j)$ is the frequency of the phonon $\vec{k}j$. The phonons leaving dS will travel across and along the rod and eventually strike the surface. Let the distance they travel down the rod before they hit the surface be denoted by $\lambda_3(\vec{k}jX_1)$. Consider now the energy flowing to the right past the plane $X_3=0$ (Fig. 5). This will be the sum of the energies of the phonons radiated by all surface elements dS to the left of the plane, provided these phonons have sufficiently long mean free paths $\lambda_3(\vec{k}jX_1)$ along the rod to pass the plane. The energy flow to the right is thus

$$Q_R=\sum_{\vec{k}j}\int_{X_1}\int_{X_3=-\infty}^{0}\hbar\omega(\vec{k}j)\vec{n}(X_1)\cdot\vec{v}(\vec{k}j)N(\vec{k}jX_3)\times\theta[\lambda_3(\vec{k}jX_1)+X_3]\,dX_1\,dX_3 \quad , \tag{6}$$

where we have used the Heaviside step function defined by

$$\theta(X)=1 \quad , \quad X\geq 0$$
$$=0 \quad , \quad X<0 \quad .$$

The integral over X_1 extends around the circumference of the rod. The X_3 integration is from $-\infty$ to 0 only when the rod is infinitely long. We consider this case first and will obtain a correction to the heat flow for a finite length rod later. The energy flow to the left may similarly be written

$$Q_L=\sum_{\vec{k}j}\int_{X_1}\int_{X_3=0}^{\infty}\hbar\omega(\vec{k}j)\vec{n}(X_1)\cdot\vec{v}(\vec{k}j)N(\vec{k}jX_3)\times\theta[-\lambda_3(\vec{k}jX_1)-X_3]\,dX_1\,dX_3 \quad . \tag{7}$$

Assuming the temperature gradient is small and uniform, we have

$$T(X_3)=T(0)+\left.\frac{\partial T}{\partial X_3}\right|_0 X_3 \quad , \tag{8}$$

$$N(\vec{k}jX_3)=N(\vec{k}j0)+\frac{\partial N(\vec{k}j)}{\partial T}\left.\frac{\partial T}{\partial X_3}\right|_0 X_3 \quad . \tag{9}$$

If Eq. (9) is inserted into the expressions for Q_R and Q_L and the integrals over X_3 are performed, then we find that the net heat flow to the right is

$$Q=Q_R-Q_L=-\frac{1}{2}\left.\frac{\partial T}{\partial X_3}\right|_0\sum_{\vec{k}j}\hbar\omega(\vec{k}j)\frac{\partial N(\vec{k}j)}{\partial T}\times\int_{X_1}\vec{n}(X_1)\cdot\vec{v}(\vec{k}j)\lambda_3^2(\vec{k}jX_1)\,dX_1 \quad . \tag{10}$$

Hence, the thermal conductivity as usually defined is

$$\kappa=\frac{1}{2A}\sum_{\vec{k}j}\hbar\omega(\vec{k}j)\frac{\partial N(\vec{k}j)}{\partial T}\int_{X_1}\vec{n}(X_1)\cdot\vec{v}(\vec{k}j)\lambda_3^2(\vec{k}jX_1)\,dX_1 \quad , \tag{11}$$

where A is the cross-sectional area. For not too complicated shapes of the cross section, the integral over X_1 may be performed analytically. For a circular rod the integral has the value

$$I=\tfrac{1}{3}(16R^3)v_3^2(\vec{k}j)/[v^2(\vec{k}j)-v_3^2(\vec{k}j)]^{1/2} \quad , \tag{12}$$

where R is the radius of the specimen and $v_3(\vec{k}j)$ is the component of $\vec{v}(\vec{k}j)$ in the direction of the rod axis. For a rectangular rod with side dimensions D and nD the integral is

$$I=\frac{D^3v_3^2(\vec{k}j)}{3v_1^2(\vec{k}j)}[3n^2|v_1(\vec{k}j)|-n^3|v_2(\vec{k}j)|], \quad |v_1(\vec{k}j)|>n|v_2(\vec{k}j)|$$
$$=\frac{D^3v_3^2(\vec{k}j)}{3v_2^2(\vec{k}j)}[3n|v_2(\vec{k}j)|-|v_1(\vec{k}j)|], \quad |v_1(\vec{k}j)|<n|v_2(\vec{k}j)| \tag{13}$$

where $v_1(\vec{k}j)$ and $v_2(\vec{k}j)$ are the components of the group velocity parallel to the sides having lengths nD and D, respectively.

Having performed the integrals over X_1 we are left with the summation over $\vec{k}j$. For isotropic solids this may be performed analytically and for square and circular cross-section rods the results obtained agree with Casimir's [see Eq. (2)]. For

a rod with rectangular cross section, the conductivity is also given by an equation of the form of Eq. (2) and in this case it can be shown that

$$\Lambda_c=(\tfrac{1}{4}Dn^{1/2})\{3n^{1/2}\ln[n^{-1}+(n^{-2}+1)^{1/2}] + 3n^{-1/2}\ln[n+(n^2+1)^{1/2}] - (n+n^3)^{1/2}+n^{3/2}-(n^{-1}+n^{-3})^{1/2}+n^{-3/2}\} \quad . \tag{14}$$

For anisotropic crystals, the summation over $\vec{k}$ and j in Eq. (11) must be performed numerically. We have done this[10] for silicon, calcium fluoride, and a number of other cubic crystals and the results are shown in Tables I and II. We have presented the results as the theoretical mean free path Λ_{theor} for an infinite length crystal defined by

$$\Lambda_{\text{theor}}=3\kappa_{\text{theor}}\langle s^{-3}\rangle/(C_{\text{theor}}\langle s^{-2}\rangle) \quad . \tag{15}$$

Here κ_{theor} is the thermal conductivity calculated theoretically from Eq. (11) and C_{theor} is the theoretical specific heat given by

$$C_{\text{theor}}=(2\pi k_B^4/5\hbar^3)\langle s^{-3}\rangle T^3 \quad . \tag{16}$$

C_{theor} was also calculated and is included in Table II.

The above analysis only applies to the conductivity in an infinitely long crystal. For a finite length crystal it is necessary to take into account the phonons which are emitted or absorbed by the end faces of the crystal. One way to proceed is to calculate explicitly the contributions to Q_R and Q_L from these phonons and to include these in the net heat flow. A simpler method[4] which gives the same result is to replace the actual finite crystal by an "equivalent infinite crystal" having a temperature distribution of the form shown by the solid line in Fig. 6. The infinite length of crystal to the left of $X_3=-L/2$ radiates phonons to the right of $X_3=-L/2$ in exactly the same way as the "black" left end face of the real finite crystal does. Q_R and Q_L are then still given by Eqs. (6) and (7) but now

$$N(\vec{k}jX_3)=N(\vec{k}\ j)+\frac{\partial N(\vec{k}j)}{\partial T}[T(X_3)-T(0)], \tag{17}$$

where

$$T(X_3)=T(0)+\frac{\partial T}{\partial X_3}\bigg|_0\frac{L}{2}, \qquad X_3>L/2$$
$$=T(0)+\frac{\partial T}{\partial X_3}\bigg|_0 X_3, \quad -L/2\le X_3\le L/2$$
$$=T(0)-\frac{\partial T}{\partial X_3}\bigg|_0\frac{L}{2}, \qquad X_3<-L/2 \quad .$$

The calculation of Q and κ is then straightforward and the result is that, compared to the infinite length crystal, the conductivity is *reduced* by

$$\Delta\kappa=\frac{1}{2A}\sum_{\vec{k}j}{}'\ \hbar\omega(\vec{k}j)\frac{\partial N(\vec{k}j)}{\partial T}\int_{X_1}\vec{n}(X_1)\cdot\vec{v}(\vec{k}j) \times[|\lambda_3(\vec{k}jX_1)|-L/2]^2dX_1 \quad , \tag{18}$$

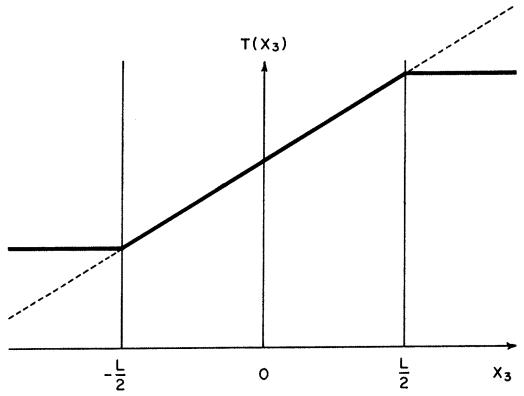

FIG. 6. Temperature distribution in the "equivalent infinite crystal" discussed in the text (heavy solid line). The temperature distribution in an infinite crystal is indicated by the dotted line.

where the prime on the summation indicates that only those phonons with mean free paths such that $|\lambda_3(\vec{k}jX_1)|>L/2$ are to be included in the summation. These phonons are the only ones contributing to the end effect correction because other phonons do not have a sufficiently long mean free path to reach the plane $X_3=0$ from the end faces of the rod.

The integral over X_1 may be performed analytically for circular, square, and rectangular cross-section samples and then the sum over $\vec{k}j$ must be carried out numerically. We have done this for each of the six silicon and three calcium fluoride crystals used in the experiments and have thus obtained a corrected theoretical conductivity. The results are shown in Table I expressed as a corrected theoretical mean free path Λ_{corr}. The length of the crystal used in these calculations was the distance between the heater and sink.

IV. DISCUSSION

The agreement between Λ_{corr}, the theoretical mean free path corrected by the end effect, and Λ_{expt}, the experimentally determined mean free path, is very good (see Table I). For the nine crystals measured, the difference between theory and experiment is never greater than 8%, and for six of the crystals is less than 4%. This is particularly satisfactory since there are no adjustable parameters in the theory, the only ingredients being the dimensions of the crystal, the elastic constants, and the density. It is interesting that this agreement is obtained without having to invoke the possibility of any degree of specular reflection of phonons at the crystal surfaces. One might expect that specular reflection would become more likely at lower temperatures. There is some indication of this in our experiments since the conductivity of calcium fluoride does not exhibit an exact T^3

temperature dependence even at the lowest temperatures investigated. For example, the ⟨110⟩ direction varies as $T^{2.8}$. Thus if we had used the conductivity at 2.5 °K to calculate the experimental mean free path Λ_{expt}, we would have obtained a result approximately 4% higher than the value given for Λ_{expt} in Table I. In the case of silicon, the conductivity varies as T^3, to within experimental uncertainty, below 3.5 °K.

We note that the agreement between theory and experiment for the ⟨111⟩ axis samples is as good as for the ⟨100⟩ and ⟨110⟩ crystals. This strongly suggests that assuming the isothermals to be planes normal to the rod axis (see Sec. III) does not lead to serious error even when it is not rigorously justifiable.

Hurst and Frankl[8] attempted to explain the anisotropy in the conductivity of silicon that they observed by invoking specular reflection. This was assumed to be larger for the ⟨100⟩ than for the ⟨110⟩ and ⟨111⟩ axis rods. They stress that to explain their observations in this way one has to assume that the degree of specularity depends on the heat flux direction and not on the crystallographic orientation of the side faces of the sample. This assumption was necessary because experimentally the conductivity of ⟨100⟩ axis square cross-section rods is approximately independent of whether the side faces are {100} or {110}. As Hurst and Frankl point out, it is rather hard to understand why the specular reflection should be dependent upon the heat flow direction and it is proposed here that the present interpretation in terms of phonon focusing due to elastic anisotropy is the correct one.

We note that the experimental results can indeed be understood in terms of the focusing concepts discussed in the Introduction. For silicon the heat-pulse experiments of Pomerantz and von Gutfeld[11] have been interpreted[6] as evidence of very strong focusing of transverse waves in the ⟨100⟩ directions. Unpublished computer calculations by Taylor[12] show that transverse wave focusing also occurs for all directions lying in {100} planes, and that there is a low intensity of transverse phonons near the ⟨111⟩ directions. This is clearly in agreement with the experimental result that ⟨100⟩ rods have the greatest conductivity and ⟨111⟩ rods the smallest. One can also understand why a rectangular cross-section rod with [110] axis has a larger conductivity if its wide side faces are (001) than if the narrow side faces are (001). If the wide side faces are (001) the focused phonons traveling parallel to this plane will have longer mean free paths than if the narrow faces are (001). For calcium fluoride, computer calculations[12] show that strong transverse wave focusing occurs in the ⟨111⟩ directions and that the lowest intensity is in the ⟨100⟩ directions. This is also consistent with the thermal conductivity results.

Finally we note that anisotropy of the thermal conductivity in the boundary scattering regime appears to be a general property of elastically anisotropic cubic crystals. In Table II we present the results of calculations of the theoretical mean free path in a number of cubic crystals. These results are for infinitely long rods. In all cases a significant degree of anisotropy is present.

---

*Work supported in part by the National Science Foundation and by the Advanced Research Projects Agency.

[1]For a general review, see J. M. Ziman, *Electrons and Phonons* (Oxford, U.P., London, 1960); P. Carruthers, Rev. Mod. Phys. 33, 92 (1961).

[2]H. B. G. Casimir, Physica 5, 495 (1938).

[3]W. J. de Haas and T. Biermasz, Physica 5, 47 (1938).

[4]R. Berman, F. E. Simon, and J. M. Ziman, Proc. Roy. Soc. (London) 220A, 171 (1953).

[5]R. Berman, E. L. Foster, and J. M. Ziman, Proc. Roy. Soc. (London) 231A, 130 (1955).

[6]B. Taylor, H. J. Maris, and C. Elbaum, Phys. Rev. Letters 23, 416 (1969).

[7]R. L. Rosenbaum, Rev. Sci. Instr. 39, 890 (1968).

[8]W. S. Hurst and D. R. Frankl, Phys. Rev. 186, 801 (1969).

[9]Note that this value differs from that used by some previous workers [M. Moss, J. Appl. Phys. 36, 3308 (1965); J. A. Harrington and C. T. Walker, Phys. Rev. B 1, 882 (1970)]. These authors calculated the averages using the velocities of longitudinal and transverse waves in the [100] direction instead of averaging over all possible wave-vector directions.

[10]This involves calculating the phase and group velocity as a function of wave-vector direction. Since the temperature is much less than the Debye temperature, these velocities may be calculated using continuum elasticity. See, for example, M. J. P. Musgrave, Proc. Roy. Soc. (London) 226, 339 (1954); Progr. Solid Mech. 2, 63 (1961).

[11]M. Pomerantz and R. J. von Gutfeld, in *Proceedings of the International Conference on the Physics of Semiconductors, Moscow, USSR*, 1968 (Nauka Publishing Leningrad, USSR, 1968), Vol. 2, p. 690.

[12]B. Taylor (unpublished). These calculations were performed using a method similar to that described in Ref. 6.